Pharmaceutical Sciences and Drug Design
ISSN: 3062-4428
2025, Volume 5, Issue 1, Page No: 33-47

Available online at: www.galaxypub.co/page/journals

Galaxy Publication

Galaxy Publication

Network Pharmacology Integration and Experimental Verification to Elucidate the Molecular Mechanisms of Triptolide in Treating Membranous Nephropathy

Aaron Clark[1*], Henry Foster[1]

[1]Department of Pharmacognosy, Faculty of Pharmacy, University of Manchester, Manchester, UK.

***E-mail** ✉ aaron.clark.uk@gmail.com

Received: 15 November 2024; **Revised:** 28 January 2025; **Accepted:** 07 February 2025

ABSTRACT

Triptolide, a principal bioactive compound derived from Tripterygium wilfordii Hook f., has shown efficacy in treating membranous nephropathy (MN), yet its precise pharmacological mechanisms remain unclear. This study employed an integrated approach combining network pharmacology and experimental validation to systematically elucidate the molecular mechanisms underlying triptolide's therapeutic effects in MN. Potential targets of triptolide and MN-associated targets were retrieved from publicly accessible databases. A protein–protein interaction (PPI) network was constructed, followed by Gene Ontology (GO) and KEGG pathway enrichment analyses, to establish target-pathway networks and identify key therapeutic targets and pathways. Molecular docking was performed to validate interactions between triptolide and hub targets. Additionally, passive Heymann nephritis (PHN) rat models were generated to experimentally confirm the molecular mechanisms of triptolide in MN treatment. Network pharmacology analysis identified 118 overlapping targets of triptolide relevant to MN, including mTOR, STAT3, CASP3, EGFR, and AKT1. Enrichment analyses highlighted involvement of signaling pathways such as PI3K/AKT, MAPK, Ras, and Rap1 in triptolide-mediated MN therapy. Molecular docking confirmed strong binding affinities of triptolide with PIK3R1, AKT1, and mTOR. In vivo studies demonstrated that triptolide significantly reduced 24-hour urinary protein levels ($P < 0.01$) and alleviated renal injury in PHN rats. Triptolide treatment also increased serum albumin while lowering total cholesterol, triglycerides, and low-density lipoprotein levels ($P < 0.05$). Western blot analyses indicated modulation of the PI3K/AKT/mTOR pathway in the triptolide-treated group compared to PHN controls. Triptolide exhibits renoprotective and antiproteinuric effects in PHN, likely through regulation of the PI3K/AKT/mTOR signaling pathway. These findings clarify the molecular mechanisms of triptolide in MN therapy and offer a scientific foundation for further basic and clinical investigations.

Keywords: Experiment verification, Membranous nephropathy, Molecular docking, Network pharmacology, Triptolide

How to Cite This Article: Clark A, Foster H. Network Pharmacology Integration and Experimental Verification to Elucidate the Molecular Mechanisms of Triptolide in Treating Membranous Nephropathy. Pharm Sci Drug Des. 2025;5(1):33-47. https://doi.org/10.51847/X9UVmVSJ4E

Introduction

Membranous nephropathy (MN) is a glomerular disease characterized by immune deposits forming on the outer surface of the basement membrane [1]. Autoantibodies targeting two major podocyte antigens, phospholipase A2 receptor (PLA2R) and thrombospondin domain-containing 7A, have been identified in 70–80% of patients, advancing our understanding of MN pathophysiology and improving therapeutic strategies [2, 3]. Clinically and pathologically, MN is classified into primary MN (pMN) and secondary MN, the latter being associated with conditions such as lupus, hepatitis B, or malignancies [4]. pMN represents the most frequent cause of idiopathic nephrotic syndrome in adults, accounting for 30% of cases in non-diabetic patients [4]. Notably, the prevalence of MN is rising by approximately 13% annually, whereas other major glomerulopathies remain stable [5]. Environmental factors, such as exposure to particulate matter 2.5 (PM2.5), may contribute to MN incidence, as

regions in China with higher PM2.5 levels show increased rates of MN [6]. Although one-third of patients may experience spontaneous remission, MN exhibits a highly variable clinical course, and current treatments for patients with heavy proteinuria or renal failure are limited and may carry nephrotoxic risks [7]. Traditional Chinese medicine (TCM) has been recognized as effective strategies for the prevention and treatment of MN [8]. Clinical trials have demonstrated therapeutic effects of natural products, including Shenqi particle, in patients with idiopathic MN (IMN) and nephrotic syndrome [9]. Experimental studies have also provided evidence for TCM efficacy through mechanisms such as regulation of nuclear factor κB (NF-κB) signaling and reduction of podocyte apoptosis [10, 11].

Tripterygium wilfordii Hook f. (TWHF) was first documented by Mao Lan in Dian Nan Ben Cao in 1476. In recent years, TWHF tablets or Tripterygium hypoglaucum Hutch tablets have been marketed in China for the treatment of autoimmune disorders and inflammatory diseases [12]. Triptolide, the principal active compound, was first isolated from TWHF in 1972 [13] and has since been used in clinical therapy [14]. Due to its multiple metabolites and well-documented anti-inflammatory and immunosuppressive properties [15], triptolide and its extracts have attracted attention for treating kidney diseases, autoimmune disorders, and rheumatoid arthritis [16]. Specifically, in MN, both in vitro and in vivo studies have shown that triptolide can protect podocytes from damage induced by puromycin aminonucleoside and reduce proteinuria [17]. Additionally, triptolide ameliorates severe proteinuria and shields against C5b-9-mediated podocyte injury in passive Heymann nephritis (PHN) models [18]. Clinical trials further support its efficacy in lowering proteinuria and improving complete remission (CR) rates in pMN patients [19]. A network meta-analysis of 13 immunosuppressive agents revealed that combining tacrolimus with triptolide is more effective than other immunosuppressants regarding CR and proteinuria reduction [20]. Despite these findings, the molecular mechanisms underlying triptolide's effects on MN remain incompletely understood. In this study, we integrated network pharmacology with molecular docking to identify potential targets of triptolide against MN and employed the PHN model to experimentally validate its pharmacological mechanisms.

Materials and Methods

Identification of triptolide structure and potential targets

The two-dimensional structure of triptolide was obtained from PubChem (https://pubchem.ncbi.nlm.nih.gov/). Its physicochemical properties were retrieved from the TCMSP database (http://tcmspw.com/). Potential targets of triptolide were collected from STITCH (http://stitch.embl.de/), Super-PRED (https://prediction.charite.de/index.php), CHEMBL (https://www.ebi.ac.uk/chembl/), and PharmMapper (http://lilab.ecust.edu.cn/), selecting "Homo sapiens" as the species. All identified targets were standardized using the UniProt database (https://www.uniprot.org/) to confirm their gene names and IDs.

Screening of MN-related targets

MN-associated targets were obtained from GeneCards (https://www.genecards.org/), DisGeNET (http://www.disgenet.org/home/), OMIM (http://www.omim.org), and DrugBank (https://go.drugbank.com/). These public databases are openly accessible and allow unrestricted reuse; therefore, ethics approval was waived (Ethics Committee of Dongzhimen Hospital, Beijing University of Chinese Medicine). The keywords "Membranous Nephropathy" and "Membranous Glomerulopathy" were used, and targets were filtered using median relevance scores. Duplicates were removed to yield the final set of MN-related targets.

Construction of the protein–protein Interaction (PPI) network

The overlap between triptolide-related targets and MN-related targets was visualized using a Venn diagram. Core regulatory genes were identified through PPI analysis using the STRING database (https://cn.string-db.org/) with an interaction score threshold of 0.4, limited to "Homo sapiens." Network topology analysis was performed using Cytoscape 3.9.1 (http://cytoscape.org/.ver.3.9.1), and high-relevance targets were screened using the CytoHubba plugin with the MCC algorithm for scoring genes [21].

GO and KEGG enrichment analyses

To explore the signaling pathways and pharmacological mechanisms of triptolide against MN, KEGG pathway enrichment analyses were conducted using Metascape (https://metascape.org/) for "Homo sapiens" with criteria:

minimum overlap = 3, P < 0.01, and minimum enrichment = 1.5. The top 25 enriched KEGG pathways were visualized using Bioinformatics (http://www.bioinformatics.com.cn/). GO enrichment analysis for biological processes (BP), cellular components (CC), and molecular functions (MF) was performed using the "clusterProfiler" R package (version 4.0.1) with parameters: pvalueCutoff = 0.05, padjustMethod = "BH", qvalueCutoff = 0.05, minGSSize = 3, maxGSSize = 500. The top 10 enriched GO terms were visualized using the "ggplot" package in R.

Construction of the target-pathway network

The target-pathway network for triptolide against MN was constructed using Cytoscape, where nodes represented the targets and triangular nodes represented the associated signaling pathways, allowing visualization of the molecular mechanisms underlying triptolide's effects on MN.

Compound-target molecular docking

To investigate the molecular interactions between triptolide and its key protein targets, molecular docking simulations were conducted. The 2D chemical structure of triptolide was downloaded in SDF format from PubChem (https://pubchem.ncbi.nlm) and converted into a 3D conformation. The ligand structure was energy-minimized using Chem3D software to achieve the most stable configuration. Corresponding protein structures were retrieved from the PDB database (https://www.rcsb.org/) and prepared in PyMOL 2.5.2 (https://pymol.org/2/) by removing bound water molecules and small ligands. The prepared ligands and receptor proteins were imported into AutoDockTools 1.5.7, where hydrogen atoms were added and water molecules removed. Grid boxes were constructed to encompass the entire receptor binding site, and semi-flexible docking simulations were performed to assess ligand-protein interactions. The docking pose with the lowest binding free energy was selected for visualization and analysis using PyMOL.

PHN model establishment and drug administration

Forty male Sprague-Dawley rats (weight range: 210–230 g) were supplied by Beijing Vital River Laboratory Animal Technology Co., Ltd. (Certificate No. SCXK (JING) 2021—0011). Animals were housed under specific pathogen-free conditions with a controlled temperature of 25 ± 2 °C, 65% humidity, and a 12-hour light/dark cycle in the Experimental Animal Centre of Dongzhimen Hospital (Certificate No. SYXK (JING) 2020—0013). All procedures adhered to national animal welfare regulations and were approved by the Animal Ethics Committee of Dongzhimen Hospital (approval No. 21–32).

PHN was induced by tail vein injection of sheep anti-rat Fx1A serum (0.5 mL/100 g, PTX-002S, Probetex, San Antonio, USA). Twenty-four-hour urine was collected using metabolic cages, and urinary protein was quantified with enzymatic kits (Nanjing Jiancheng Bioengineering Institute, Nanjing, China). Triptolide (purity 99.6%, Batch No. 111567-202005, Chinese National Institute for Control of Pharmaceutical and Biological Products, Beijing, China) was dissolved in 0.01% dimethyl sulfoxide and administered orally at 200 mg/kg/day beginning 10 days after PHN induction, once proteinuria was established. Thirty PHN rats were randomly divided into three groups: PHN model group (n = 10) received 0.01% DMSO in water, triptolide-treated group (n = 10) received 200 mg/kg/day triptolide, and positive control group (FK506, n = 10) received 1 mg/kg/day FK506. Dosing was adjusted from human equivalent doses according to international guidelines. Ten healthy rats served as normal controls. Treatment continued for 50 days.

Urine and serum biochemical analysis

Rats were transferred to metabolic cages every 10 days for 24-hour urine collection with unrestricted water access but no food. At the end of the 50-day treatment period, animals were fasted for 12 hours and euthanized via intraperitoneal injection of 35 mg/kg pentobarbital sodium. Blood was collected from the abdominal aorta, centrifuged at 3000 rpm for 10 min, and serum was analyzed for albumin (ALB), total cholesterol (TC), triglycerides (TG), and low-density lipoprotein (LDL) using commercial kits (Nanjing Jiancheng Bioengineering Institute, Nanjing, China). Urinary protein levels were measured using the same manufacturer's protocols.

Renal histopathology

Kidneys were fixed in 4% paraformaldehyde (P1110, Solarbio), dehydrated in graded ethanol, and embedded in paraffin. Sections (3 μm) were prepared for staining with hematoxylin and eosin (H&E), periodic acid–Schiff

(PAS), and periodic acid–silver methenamine (PASM). Histopathological changes were observed under a light microscope at 400× magnification (BX60, Olympus, Tokyo, Japan).

Immunofluorescence assay

Paraffin kidney sections (3 μm) were baked at 60 °C for 60 min, deparaffinized in xylene, rehydrated through graded alcohols, and subjected to antigen retrieval. Sections were permeabilized with 0.2% PBST for 20 min, blocked with 5% donkey serum at 37 °C for 30 min, and incubated overnight at 4 °C with anti-synaptopodin antibody (sc515842, Santa Cruz, USA). After washing, sections were incubated with Alexa Fluor® 488 donkey anti-rabbit IgG (lot 1927937, Thermo Fisher Scientific) at 37 °C for 60 min and counterstained with DAPI (ZLI-9557, ZSGB-Bio).

Immunohistochemistry assay

Sections (3 μm) were baked, deparaffinized, rehydrated, and subjected to citrate-based antigen retrieval at 95 °C for 20 min. Endogenous peroxidase activity was blocked with 3% hydrogen peroxide, followed by 60 min of goat serum blocking. Sections were incubated overnight at 4 °C with desmin antibody (ab32362, Abcam, UK), then with secondary antibody at 37 °C for 30 min. Sections were developed with DAB, counterstained with hematoxylin, and quantified using Image-Pro Plus 6.0 software for integral optical density (IOD).

Western blot analysis

Proteins from the renal cortex were extracted using lysis buffer containing protease inhibitors and quantified via BCA assay (BN27109-500T, Biorigin, Beijing, China). Proteins were separated on 10% SDS-PAGE gels, transferred to nitrocellulose membranes, blocked with 5% skim milk in TBST for 1 h, and incubated overnight at 4 °C with primary antibodies: synaptopodin (ab32127, Abcam), AKT (#4685, CST), p-AKT (#13038, CST), PI3K (#4257, CST), p-PI3K (#17366, CST), mTOR (#2983, CST), and p-mTOR (#5536, CST). Following TBST washes, membranes were incubated with HRP-conjugated secondary antibodies for 1 h. Protein bands were detected using an ECL kit (P1010, Applygen, Beijing, China) on a Tanon 5200 imaging system and quantified with Image J software.

Statistical analysis

All statistical analyses were conducted using SPSS version 20.0 (IBM, Chicago, IL, USA). Data are presented as mean ± standard deviation (SD). Comparisons among multiple groups were performed using one-way ANOVA, and a p-value less than 0.05 was considered statistically significant. Graphical representations were created using GraphPad Prism 8.0 (San Diego, CA, USA).

Identification of triptolide targets against MN

The 2D chemical structure of triptolide is shown in **Figure 1a**, with its physicochemical properties summarized in **Table 1**. Using STITCH, Super-PRED, CHEMBL, and PharmMapper databases, 435 unique potential targets for triptolide were predicted after removal of duplicates and standardized via the UniProt database to confirm Gene names and IDs. For MN-associated genes, the top 25% of target genes from GeneCards were selected based on relevance scores and combined with targets from DisGeNET, OMIM, and DrugBank databases, yielding 1,347 unique MN-related targets. Intersecting the 435 triptolide-related targets with the 1,347 MN-related targets through a Venn diagram identified 118 overlapping targets, which were considered as the key therapeutic targets of triptolide against MN **(Figure 1b)**.

Table 1. Chemical Information of the Active Compounds of Triptolide

Name	The Number of Hydrogen Bonds	Amino Acid Residue	Target	Binding Energy/kcal mol^{-1}
Triptolide	1	ASN-204	AKT1	−8.42
	2	VAL-2183	mTOR	−6.16
		ALA-2226		
	2	TYR-12 TYR-76	PIK3R1	−5.87

a) b)

Figure 1. (a) The 2D structure of triptolide. (b) Venn diagram of the overlapping genes of triptolide and MN.

Protein–protein Interaction (PPI) network analysis of triptolide targets against MN

To elucidate the potential pharmacological mechanisms of triptolide in MN, the 118 overlapping targets were analyzed using the STRING database to construct a protein–protein interaction (PPI) network. Subsequent topological analysis was performed in Cytoscape software **(Figure 2a)**. Using the MCC algorithm, the ten most central hub proteins were identified: mTOR, STAT3, CASP3, EGFR, AKT1, HIF1A, MMP9, SRC, HRAS, and HSP90AA1 **(Figure 2b)**. These proteins were considered core targets mediating triptolide's therapeutic effects and were selected for further molecular docking studies.

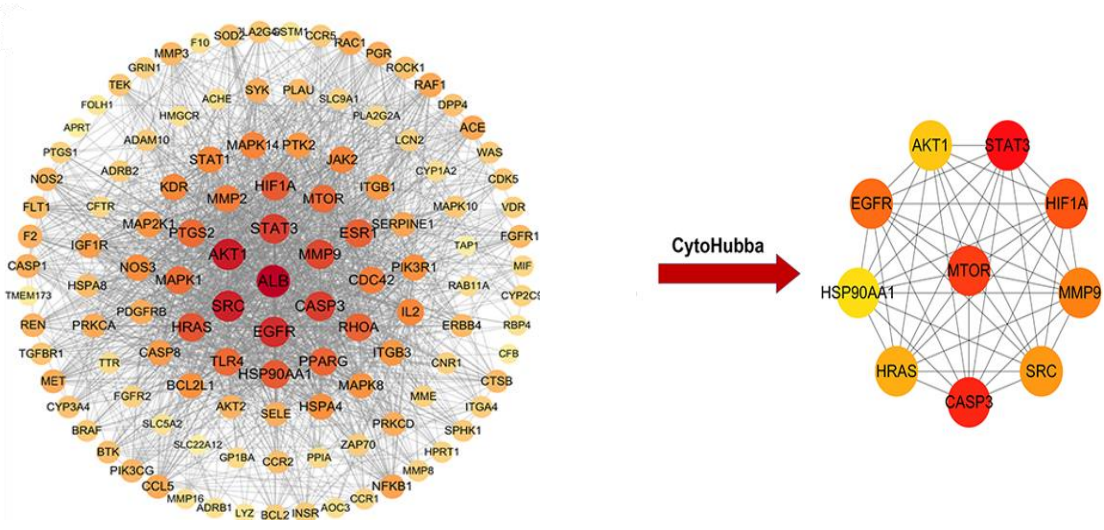

a) b)

Figure 2. Protein–Protein Interaction Network of Triptolide Targets in MN

(a) A PPI network comprising 118 intersecting targets of triptolide against MN was constructed using STRING, consisting of 118 nodes connected by 1,729 edges. The relative node size and color intensity indicate the degree of connectivity within the network. (b) Hub proteins with the highest MCC scores, including mTOR, STAT3, CASP3, EGFR, AKT1, HIF1A, MMP9, SRC, HRAS, and HSP90AA1, were identified as key mediators of triptolide's therapeutic action and selected for further molecular docking studies.

GO and KEGG enrichment analysis

To uncover the potential molecular mechanisms through which triptolide acts in MN, the 118 overlapping targets were subjected to KEGG pathway analysis via Metascape, revealing a total of 190 pathways. The top 25 pathways, ranked by statistical significance, were visualized in bar and circular plots **(Figures 3a and 3b)** to highlight the

most relevant signaling cascades. Notably, PI3K/AKT, MAPK, Ras, Rap1, and cancer-related pathways emerged as central mediators of triptolide's effects in MN.

GO functional enrichment further classified 1,604 biological processes (BPs), 113 cellular components (CCs), and 152 molecular functions (MFs) **(Figures 3c and 3e)**. Key biological processes included regulation of cell migration, mobilization of cellular components, and general cell motility. Cellular components were predominantly associated with focal adhesions and cell-substrate junctions. In the molecular function category, targets were enriched for kinase activity, particularly protein serine/threonine/tyrosine kinase activity, indicating that triptolide may exert its renoprotective effects by modulating critical intracellular signaling events.

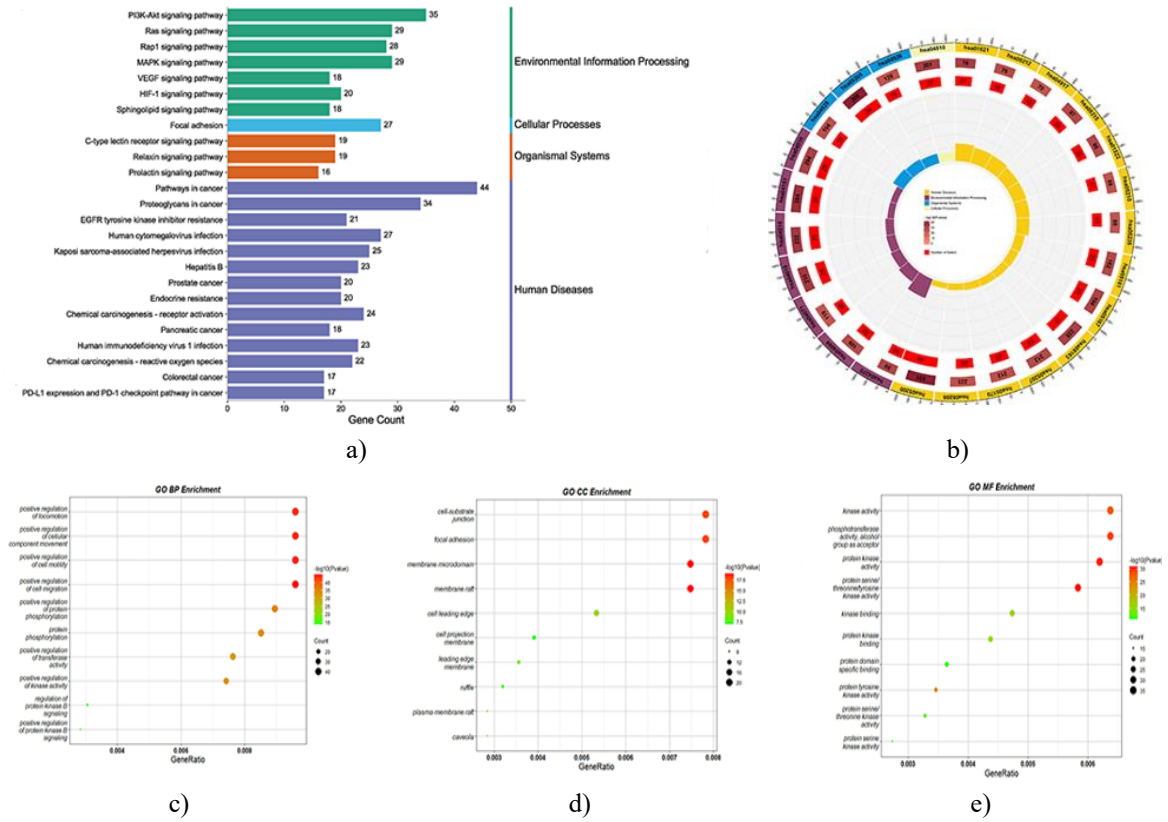

Figure 3. GO and KEGG pathway enrichment analysis of triptolide in the treatment of MN. (a) KEGG pathway enrichment results, where the X-axis represents the number of genes associated with each pathway, and varying colors denote different KEGG pathway categories. (b) KEGG pathway circle plot: the outermost circle displays the classification of enriched pathways with a coordinate scale indicating the number of genes, while different colors correspond to specific classifications; the second circle presents the number of genes in that category from the background and their P-values; the third circle indicates the total number of foreground genes annotated to each pathway; and the fourth circle shows the Rich-Factor for each classification, with each grid line of the background representing 0.1. (c–Ee) GO enrichment analysis of the key targets. Abbreviations: BP, biological process; CC, cellular component; MF, molecular function.

Target-pathway network

A target-pathway network was established based on pathways associated with the target genes **(Figure 4a)**, encompassing 118 target genes across 10 pathways. To clarify the potential pharmacological mechanisms of triptolide against MN, a network integrating the top 10 signaling pathways with the 118 targets was constructed. By combining drug core target analysis, functional enrichment, and the target-pathway network, we determined that triptolide predominantly exerts its effects through the PI3K-AKT signaling pathway. To further illustrate the interaction between triptolide and the PI3K-AKT pathway, a subnet was extracted showing its mapping to hub genes **(Figure 4b)**, identifying five core targets, with the PI3K/AKT signaling pathway as a major mediator of triptolide's action.

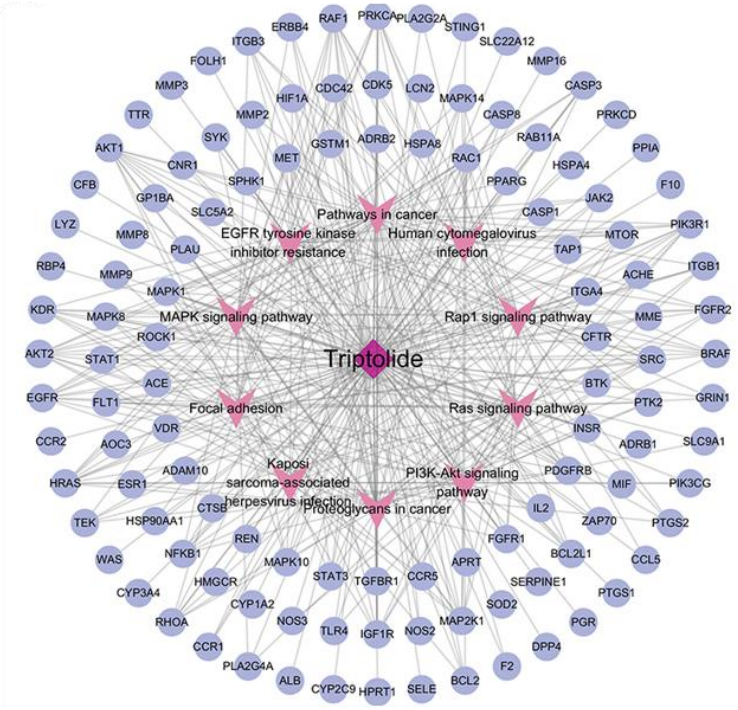

a)

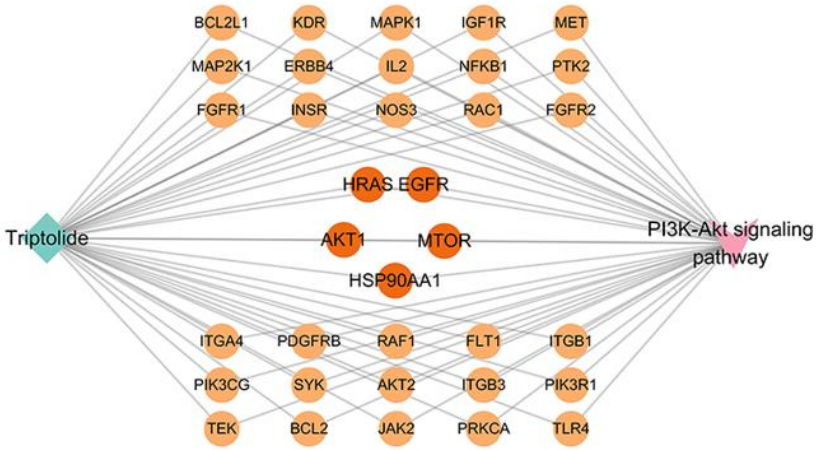

b)

Figure 4. "Target-Pathway" network of triptolide in MN treatment. (a) In the network, circular nodes represent target genes, while triangular nodes indicate the associated signaling pathways of triptolide and MN. (b) Enrichment of triptolide targets within the PI3K/AKT signaling pathway, where dark orange nodes represent the top 10 targets identified by MCC score along with the PI3K/AKT pathway.

Molecular docking analysis

Molecular docking was performed to explore the interaction modes between triptolide and its targets. Binding energy serves as an indicator of the ligand-receptor interaction strength; lower values signify stronger and more stable binding. Triptolide was docked individually with three protein targets **(Table 2)**. As the structure of PI3K is unavailable in the PDB database, PIK3R1, the regulatory subunit of PI3K, was used for analysis. The triptolide-AKT1 complex (PDB: 7NH5) formed a stable hydrogen bond with ASN204, showing a binding energy of −8.42 **(Figure 5a)**. The triptolide-mTOR complex (PDB: 3JBZ) established two hydrogen bonds with VAL2183 and ALA2226, yielding a binding energy of −6.16 **(Figure 5b).** The triptolide-PIK3R1 complex (PDB: 3I5S) interacted via two hydrogen bonds with TYR12 and TYR76, with a binding energy of −5.87 **(Figure 5c)**. The favorable binding energies of these three complexes indicate strong interactions, supporting the pharmacological network predictions for triptolide.

Table 2. Virtual Molecular Docking of Triptolide and Its Targets

Name	The Number of Hydrogen Bonds	Amino Acid Residue	Target	Binding Energy/kcal mol^{-1}
Triptolide	1	ASN-204	AKT1	−8.42
	2	VAL-2183	mTOR	−6.16
		ALA-2226		
	2	TYR-12 TYR-76	PIK3R1	−5.87

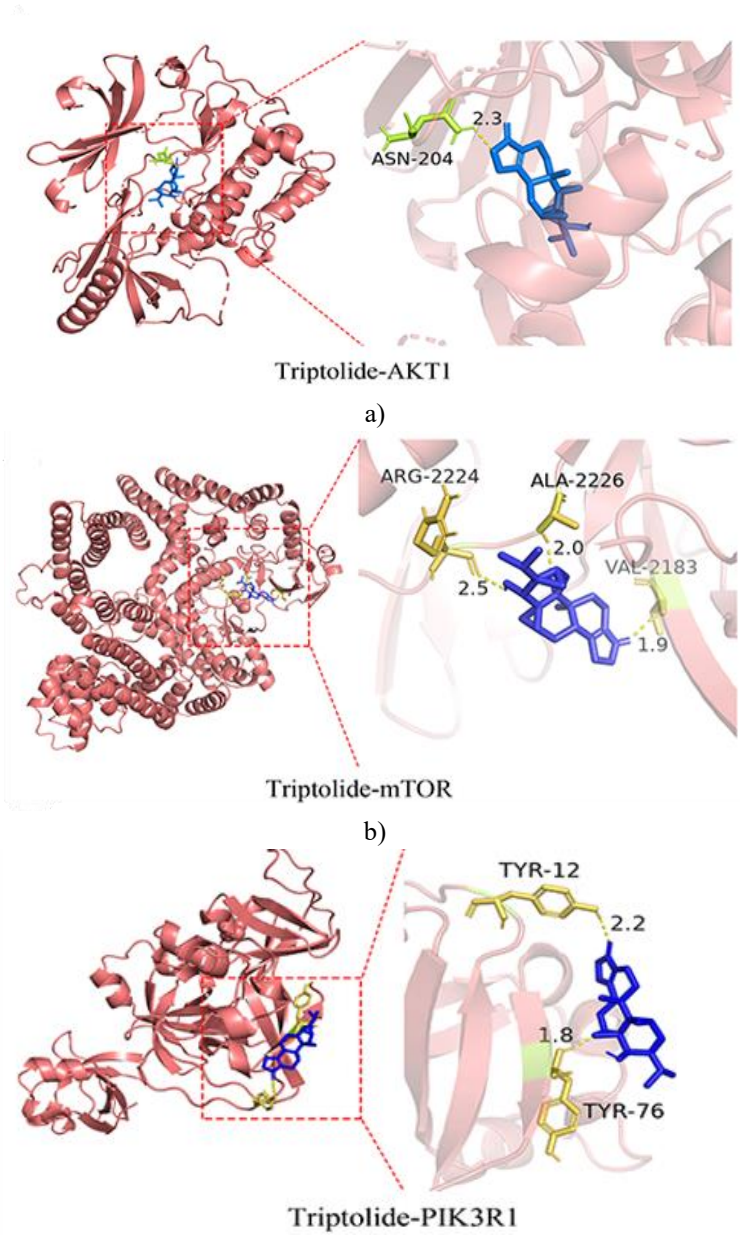

Figure 5. 3D molecular docking of triptolide with AKT1 (a), mTOR (b), and PIK3R1 (c), with numbers indicating hydrogen bond distances.

Effect of triptolide on biochemical indicators in PHN rats

Administration of triptolide significantly lowered the 24-hour urinary total protein (24hUTP) in PHN rats. PHN rats initially displayed elevated 24hUTP levels compared to normal controls, but treatment with triptolide led to a notable decrease on days 20, 30, 40, and 50 ($P < 0.01$). Importantly, after 20 days, the reduction in urinary protein achieved by triptolide was equivalent to that observed with FK506 **(Figure 6a)**.

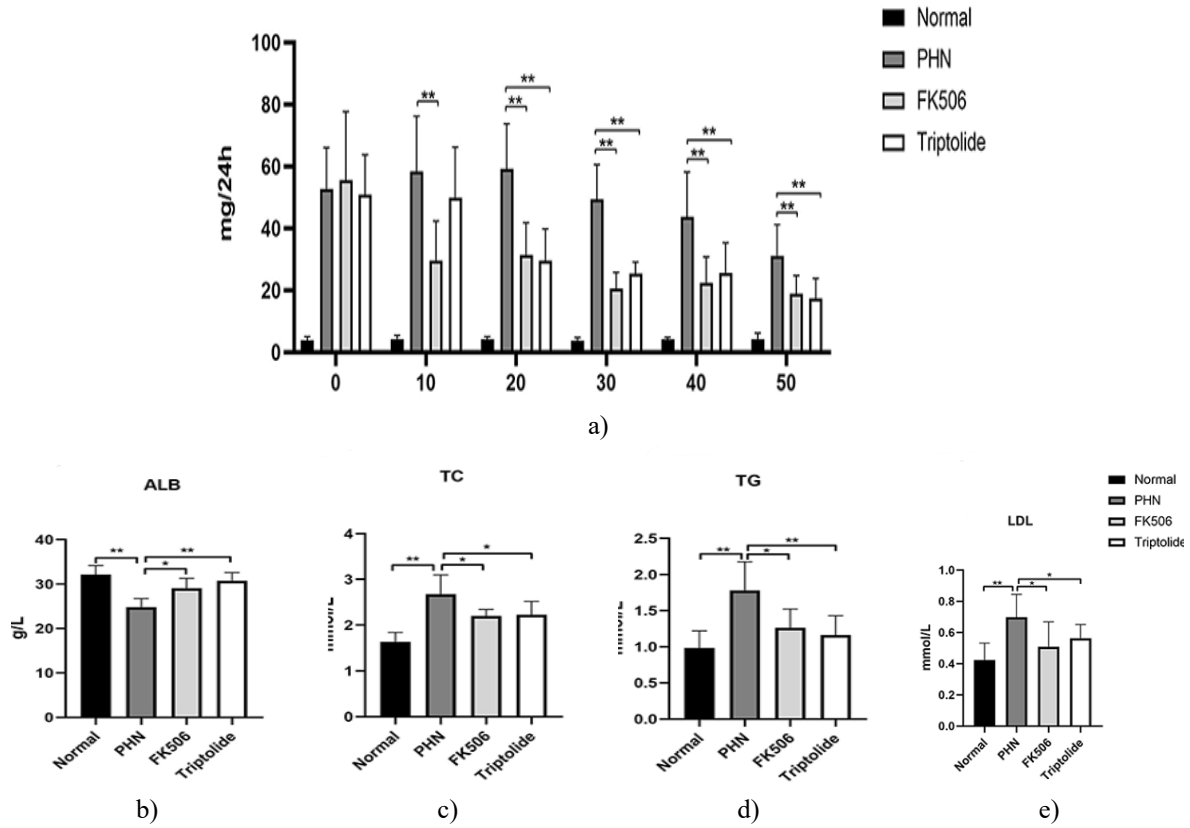

Figure 6. The impact of triptolide on the biochemical parameters of PHN rats. (a) shows the 24-hour urine protein levels (n = 10), while (b–e) display serum levels of ALB, TC, TG, and LDL during the final week (n = 10). *p < 0.05, **p < 0.01.

In line with the pronounced proteinuria observed, serum ALB levels were markedly higher in normal control rats than in PHN rats ($P < 0.01$). Treatment with triptolide significantly increased serum ALB levels compared with untreated PHN rats ($P < 0.01$), producing effects comparable to FK506 **(Figure 6b).**
Additionally, PHN rats exhibited elevated blood lipid levels relative to normal controls ($P < 0.01$). Administration of triptolide effectively reduced serum lipid levels, including TC, TG, and LDL, compared with untreated PHN rats ($P < 0.05$) **(Figurs 6c and 6e)**.

Triptolide mitigates renal Injury in PHN rats
PHN rats demonstrated glomerular enlargement, basement membrane thickening, protein casts, and mild inflammatory infiltration **(Figure 7)**. Rats treated with triptolide or FK506 showed marked improvements in these renal pathological features compared with untreated PHN rats.

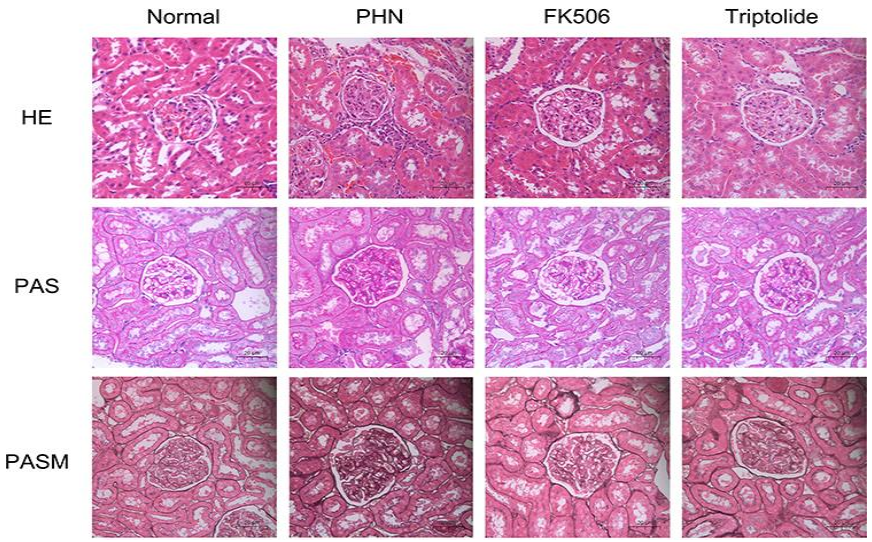

Figure 7. The impact of triptolide on renal histopathology in PHN rats. Representative kidney sections were stained with H&E, PAS, and PASM and examined at 400× magnification (scale bar = 20 μm).

Triptolide attenuates podocyte damage in PHN rats

Desmin serves as a marker for podocyte injury, being expressed specifically in glomeruli where podocytes are damaged. In normal control rats, desmin expression in podocytes was minimal. In contrast, PHN rats exhibited markedly increased desmin staining in podocytes **(Figure 8a)**. Administration of triptolide significantly reduced desmin expression compared with untreated PHN rats ($P < 0.01$) **(Figure 8b)**.

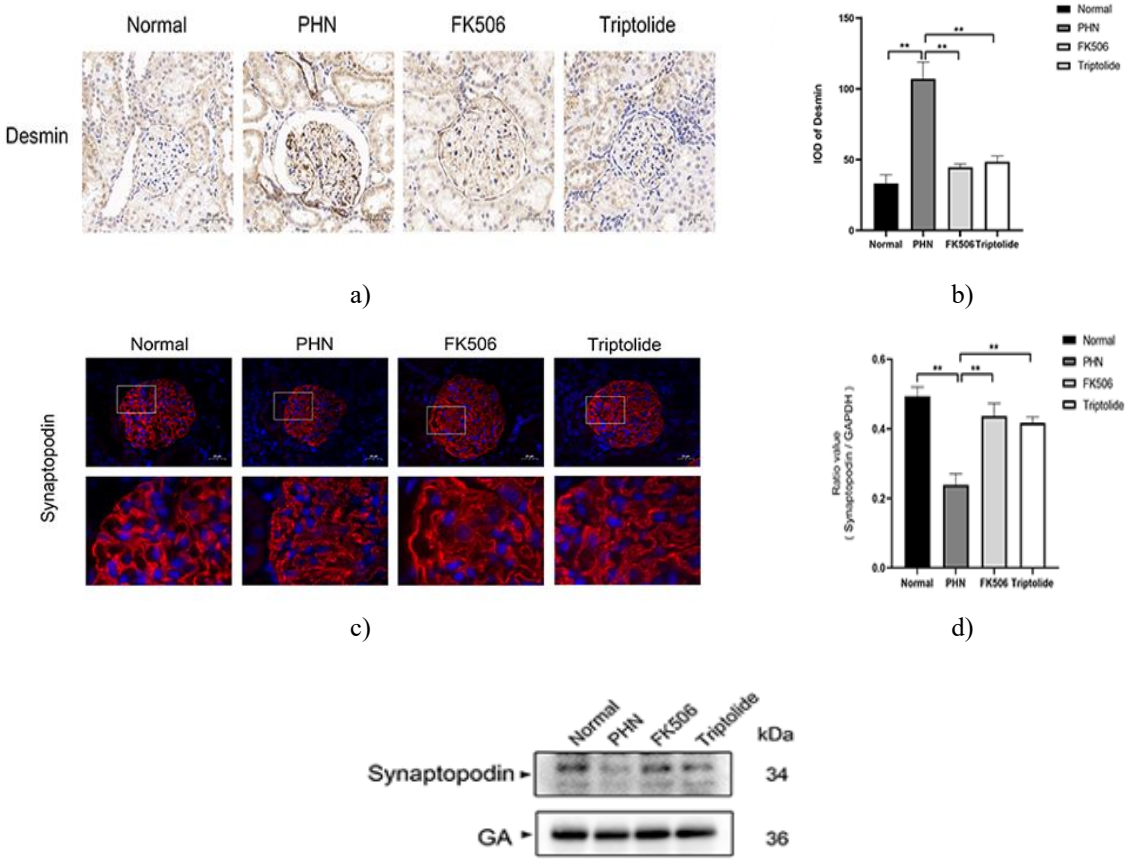

Figure 8. The effects of triptolide on podocyte injury in PHN rats. Panel (a) shows immunohistochemical staining for desmin at 400× magnification, while panel (b) presents the quantitative analysis of desmin IOD.

Panel (c) displays immunofluorescence staining for synaptopodin (400×, scale bar = 20 μm), and panels (e) and (d) show representative Western blots and the corresponding relative protein levels of synaptopodin. Data are presented as mean ± SD (n = 6). *p < 0.05, **p < 0.01.

Synaptopodin, an actin-associated protein critical for podocyte motility and glomerular filtration barrier integrity, serves as a hallmark of mature podocytes. Immunofluorescence analysis revealed that synaptopodin expression was reduced in PHN rats compared with normal controls. Treatment with triptolide substantially restored synaptopodin expression **(Figure 8c)**. These findings were corroborated by Western blot analysis, which showed a significant decrease in synaptopodin levels in PHN rats ($P < 0.01$) and a marked upregulation following triptolide treatment ($P < 0.01$) **(Figures 8e and 8c)**.

Triptolide suppresses the PI3K/AKT signaling pathway

To investigate the molecular mechanisms underlying triptolide's protective effects against MN, the PI3K/AKT pathway was examined by assessing protein levels of PI3K, AKT, and mTOR using Western blotting **(Figure 9a).** PHN rats displayed elevated levels of phosphorylated PI3K, AKT, and mTOR compared with normal controls ($P < 0.01$). Treatment with triptolide significantly reduced the phosphorylation of these signaling molecules relative to untreated PHN rats ($P < 0.05$) **(Figures 9b-9d).**

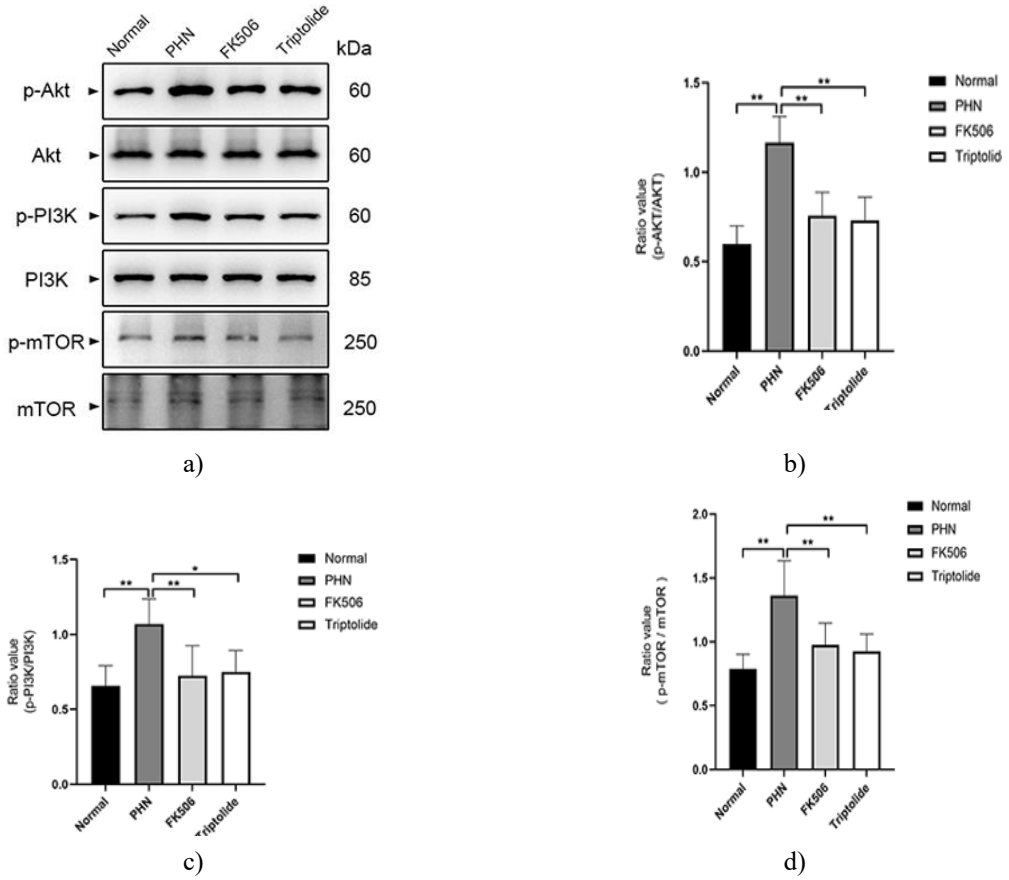

Figure 9. Validation of predicted target proteins using Western blot analysis. Panel (a) shows representative Western blots for p-AKT, AKT, p-PI3K, PI3K, p-mTOR, and mTOR. Panels (b–d) illustrate that the phosphorylation levels of AKT, PI3K, and mTOR were significantly reduced following triptolide treatment. Data are expressed as mean ± SD (n = 6). *p < 0.05, **p < 0.01.

Results and Discussion

Membranous nephropathy (MN) is an organ-specific autoimmune disorder characterized by subepithelial immune complex deposition caused by circulating autoantibodies targeting podocyte antigens [22]. Triptolide has been widely used for treating kidney diseases, particularly MN, due to its strong immunosuppressive and anti-

inflammatory effects [18, 23]. In this study, we combined network pharmacology with in vivo experimental validation to systematically investigate the mechanisms underlying triptolide's therapeutic action in MN. Comparison of 435 triptolide-related targets with 1347 MN-associated targets revealed 118 overlapping proteins. Based on the MCC score from CytoHubba, the top ten core targets were mTOR, STAT3, CASP3, EGFR, AKT1, HIF1A, MMP9, SRC, HRAS, and HSP90AA1.

Integration of network topology with GO and KEGG enrichment analyses indicated that triptolide acts through multiple targets and major signaling pathways. KEGG enrichment revealed that PI3K/AKT, MAPK, Ras, and Rap1 signaling pathways were among the top 15, while GO analysis suggested that triptolide primarily affects biological processes related to positive regulation of cell migration and cellular component movement. Previous research also demonstrated that Hydrangea paniculata exerts renal protective effects via PI3K/AKT pathway modulation [24], and Zhen-Wu-Tang improves MN-associated renal injury by inhibiting NF-κB and NLRP3 inflammasome activity [25].

To investigate triptolide's therapeutic effects, PHN, a rat model with a pathogenesis similar to MN, was induced. Triptolide treatment significantly reduced 24-hour urine protein levels and improved biochemical parameters, including serum ALB, TC, TG, and LDL. Mechanistically, triptolide decreased phosphorylation of PI3K, AKT, and mTOR in vivo, indicating that its protective effects are mediated through inhibition of this pathway.

The integrity of podocytes is maintained by an organized actin cytoskeleton forming the slit diaphragm, a key component of the glomerular filtration barrier, mainly composed of nephrin [26]. Triptolide protected against PHN-induced cytoskeletal disruption, restored synaptopodin expression, and decreased desmin levels, demonstrating its capacity to reverse podocyte injury and reduce proteinuria.

The triptolide-MN network highlighted ten core targets, several of which have been previously linked to triptolide's effects on MN, supporting the predictive value of network pharmacology. For example, mTOR, a central regulator of metabolism, can be inhibited to reduce proteinuria-induced tubulointerstitial inflammation and fibrosis in PHN [27]. CASP3 is critical for apoptosis, a hallmark of podocyte loss in MN, and triptolide has been shown to protect podocytes by suppressing apoptosis [28–30]. STAT3, a key transcription factor for Th17 cell development, is implicated in MN pathogenesis through altered Th17/Treg ratios [31], and MMP9 has been identified as a biomarker for severe proteinuria in MN patients [32].

To further clarify triptolide's mechanisms, a target-pathway network was constructed. Analysis indicated that triptolide may attenuate renal injury by modulating the PI3K/AKT signaling pathway. Most hub targets were associated with PI3K/AKT and its downstream pathways **(Figure 4)**. The PI3K/AKT pathway, involving three AKT isoforms (AKT1–3), is activated via phosphorylation at Thr308 by 3-phosphoinositide-dependent protein kinase 1, which is itself activated by PI3K, regulating cell growth, proliferation, cytoskeleton organization, and metabolism [33]. Prior studies have shown that overactivation of PI3K/AKT contributes to MN progression, including macrophage-induced renal fibrosis and podocyte apoptosis, which can be mitigated by inhibiting PI3K/AKT/mTOR signaling [25, 34, 35]. Additionally, compounds such as curcumin and salvianolic acid B improve MN by enhancing autophagy and suppressing PI3K/AKT/mTOR [35], while triptolide and related formulations, including Colquhounia root tablets and Kunxian capsules, restore immune-inflammatory balance by modulating PI3K/AKT/NF-κB/TNF-α pathways [36–38].

Molecular docking predicted stable binding of triptolide to AKT1, PIK3R1, and mTOR via hydrogen bonds, supporting direct inhibition of the PI3K/AKT/mTOR pathway. Experimental validation confirmed that triptolide modulates this pathway to protect the kidney. These findings suggest that triptolide's active components act synergistically to exert antiproteinuric and renoprotective effects.

However, this study has limitations. First, the complex pharmacological mechanisms of triptolide in MN cannot be fully elucidated here. Second, although network pharmacology and animal experiments were combined, further studies using PI3K/AKT inhibitors are needed to definitively confirm triptolide's protective effects on podocytes.

Conclusion

In this study, the pharmacological mechanisms of triptolide against MN were systematically elucidated using an integrated strategy of network pharmacology, molecular docking, and in vivo experimental validation. Triptolide displayed strong binding stability with PIK3R1, AKT1, and mTOR. The predictive potential of the triptolide-MN network was validated in PHN rats, and its therapeutic activity was shown to involve regulation of the

PI3K/AKT/mTOR pathway. In conclusion, triptolide exerts its therapeutic effects through multi-target, multi-pathway, and systemic regulatory actions.

Acknowledgments: None

Conflict of Interest: None

Financial Support: None

Ethics Statement: None

References

1. Ronco P, Debiec H. Molecular pathogenesis of membranous nephropathy. Annu Rev Pathol. 2020;15:287-313. doi:10.1146/annurev-pathol-020117-043811
2. Beck LH, Bonegio RG, Lambeau G, Beck DM, Powell DW, Cummins TD, et al. M-type phospholipase A2 receptor as target antigen in idiopathic membranous nephropathy. N Engl J Med. 2009;361(1):11-21. doi:10.1056/NEJMoa0810457
3. Tomas NM, Beck LH Jr, Meyer-Schwesinger C, Seitz-Polski B, Ma H, Zahner G, et al. Thrombospondin type-1 domain-containing 7A in idiopathic membranous nephropathy. N Engl J Med. 2014;371(24):2277-87. doi:10.1056/NEJMoa1409354
4. Couser WG. Primary membranous nephropathy. Clin J Am Soc Nephrol. 2017;12(6):983-97. doi:10.2215/CJN.11761116
5. Ronco P, Beck L, Debiec H, Fervenza FC, Hou FF, Hutchinson CA, et al. Membranous nephropathy. Nat Rev Dis Primers. 2021;7(1):69. doi:10.1038/s41572-021-00303-z
6. Xu X, Wang G, Chen N, Lu T, Nie S, Xu G, et al. Long-term exposure to air pollution and increased risk of membranous nephropathy in China. J Am Soc Nephrol. 2016;27(12):3739-46. doi:10.1681/ASN.2016010093
7. Alsharhan L, Beck LH Jr. Membranous nephropathy: core curriculum 2021. Am J Kidney Dis. 2021;77(3):440-53. doi:10.1053/j.ajkd.2020.10.009
8. Wang YN, Feng HY, Nie X, Zhang Y, Zou Y, Song X, et al. Recent advances in clinical diagnosis and pharmacotherapy options of membranous nephropathy. Front Pharmacol. 2022;13:907108. doi:10.3389/fphar.2022.907108
9. Chen Y, Deng Y, Ni Z, Chen N, Chen X, Shi W, et al. Efficacy and safety of traditional Chinese medicine (Shenqi particle) for patients with idiopathic membranous nephropathy: a multicenter randomized controlled clinical trial. Am J Kidney Dis. 2013;62(6):1068-76. doi:10.1053/j.ajkd.2013.05.005
10. Lu H, Luo Y, Su B, Dong H, Li H, Wang Y, et al. Wenyang Lishui decoction ameliorates podocyte injury in membranous nephropathy rat and cell models by regulating p53 and Bcl-2. Evid Based Complement Alternat Med. 2020;2020:6813760. doi:10.1155/2020/6813760
11. Tian R, Wang L, Chen A, Huang L, Liang X, Gao Q, et al. Sanqi oral solution ameliorates renal damage and restores podocyte injury in experimental membranous nephropathy via suppression of NFkappaB. Biomed Pharmacother. 2019;115:108904. doi:10.1016/j.biopha.2019.108904
12. Law SK, Simmons MP, Techen N, Khan IA, He MF, Shaw PC, et al. Molecular analyses of the Chinese herb Leigongteng (Tripterygium wilfordii Hook.f.). Phytochemistry. 2011;72(1):21-6. doi:10.1016/j.phytochem.2010.10.015
13. Kupchan SM, Court WA, Dailey RG Jr, Gilmore CJ, Bryan RF. Triptolide and tripdiolide, novel antileukemic diterpenoid triepoxides from Tripterygium wilfordii. J Am Chem Soc. 1972;94(20):7194-5. doi:10.1021/ja00775a078
14. Gao J, Zhang Y, Liu X, Wu X, Huang L, Gao W. Triptolide: pharmacological spectrum, biosynthesis, chemical synthesis and derivatives. Theranostics. 2021;11(15):7199-221. doi:10.7150/thno.57745
15. Bai S, Hu Z, Yang Y, Yin Y, Li W, Wu L, et al. Anti-inflammatory and neuroprotective effects of triptolide via the NF-kappaB signaling pathway in a Rat MCAO model. Anat Rec (Hoboken). 2016;299(2):256-66. doi:10.1002/ar.23293

16. Hou W, Liu B, Xu H. Medicinal chemistry, chemical biology and clinical progress of triptolide. Eur J Med Chem. 2019;176:378-92. doi:10.1016/j.ejmech.2019.05.032
17. Zheng CX, Chen ZH, Zeng CH, Qin WS, Li LS, Liu ZH. Triptolide protects podocytes from puromycin aminonucleoside induced injury in vivo and in vitro. Kidney Int. 2008;74(5):596-612. doi:10.1038/ki.2008.203
18. Chen ZH, Qin WS, Zeng CH, Zheng CX, Hong YM, Yu YS, et al. Triptolide reduces proteinuria in experimental membranous nephropathy and protects against C5b-9-induced podocyte injury in vitro. Kidney Int. 2010;77(11):974-88. doi:10.1038/ki.2010.41
19. Guo Y, Guo N, Wang J, Wang R, Tang L. Retrospective analysis of Tripterygium wilfordii polyglycoside combined with angiotensin receptor blockers for the treatment of primary membranous nephropathy with sub-nephrotic proteinuria. Ren Fail. 2021;43(1):729-36. doi:10.1080/0886022X.2021.1918555
20. Zheng Q, Yang H, Liu W, Sun J, Qian J, Fu Y, et al. Comparative efficacy of 13 immunosuppressive agents for idiopathic membranous nephropathy in adults with nephrotic syndrome: a systematic review and network meta-analysis. BMJ Open. 2019;9(9):e030919. doi:10.1136/bmjopen-2019-030919
21. Chin CH, Chen SH, Wu HH, Ho CW, Ko MT, Lin CY. cytoHubba: identifying hub objects and sub-networks from complex interactome. BMC Syst Biol. 2014;8 Suppl 4:S11. doi:10.1186/1752-0509-8-S4-S11
22. Ronco P, Debiec H. Pathophysiological advances in membranous nephropathy: time for a shift in patient's care. Lancet. 2015;385(9981):1983-92. doi:10.1016/s0140-6736(15)60731-0
23. Liu S, Li X, Li H, Liang Q, Chen J, Chen J. Comparison of tripterygium wilfordii multiglycosides and tacrolimus in the treatment of idiopathic membranous nephropathy: a prospective cohort study. BMC Nephrol. 2015;16:200. doi:10.1186/s12882-015-0199-x
24. Wang W, Sheng L, Chen Y, Li J, Zhang M, Xu J, et al. Total coumarin derivates from Hydrangea paniculata attenuate renal injuries in cationized-BSA induced membranous nephropathy by inhibiting complement activation and interleukin 10-mediated interstitial fibrosis. Phytomedicine. 2022;96:153886. doi:10.1016/j.phymed.2021.153886
25. Liu B, Lu R, Li H, Zhou Y, Xu L, Chen Y, et al. Zhen-Wu-Tang ameliorates membranous nephropathy rats through inhibiting NF-kappaB pathway and NLRP3 inflammasome. Phytomedicine. 2019;59:152913. doi:10.1016/j.phymed.2019.152913
26. Beck LH Jr, Salant DJ. Membranous nephropathy: from models to man. J Clin Invest. 2014;124(6):2307-14. doi:10.1172/JCI72270
27. Bonegio RG, Fuhro R, Wang Z, Valeri CR, Andry C, Salant DJ, et al. Rapamycin ameliorates proteinuria-associated tubulointerstitial inflammation and fibrosis in experimental membranous nephropathy. J Am Soc Nephrol. 2005;16(7):2063-72. doi:10.1681/ASN.2004030180
28. Sun Z, Xu Q, Ma Y, Yang S, Shi J. Circ_0000524/miR-500a-5p/CXCL16 axis promotes podocyte apoptosis in membranous nephropathy. Eur J Clin Invest. 2021;51(3):e13414. doi:10.1111/eci.13414
29. Yang YQ, Liang J, Han XD, Xue YJ, Yang ZY, Li Y, et al. Dual-function of triptriolide in podocytes injury: inhibiting of apoptosis and restoring of survival. Biomed Pharmacother. 2019;109:1932-9. doi:10.1016/j.biopha.2018.11.031
30. Gao J, Liang Z, Zhao F, Liu X, Ma N. Triptolide inhibits oxidative stress and inflammation via the microRNA-155-5p/brain-derived neurotrophic factor to reduce podocyte injury in mice with diabetic nephropathy. Bioengineered. 2022;13(5):12275-88. doi:10.1080/21655979.2022.2067293
31. Motavalli R, Etemadi J, Soltani-Zangbar MS, Ardalan M, Kahroba H, Roshangar L, et al. Altered Th17/Treg ratio as a possible mechanism in pathogenesis of idiopathic membranous nephropathy. Cytokine. 2021;141:155452. doi:10.1016/j.cyto.2021.155452
32. Gilbert A, An C, Chen G, Liu J, Qin X. Urinary matrix metalloproteinase-9 and nephrin in idiopathic membranous nephropathy: a cross-sectional study. Dis Markers. 2021;2021:1620545. doi:10.1155/2021/1620545
33. Qiu D, Kao PN. Immunosuppressive and anti-inflammatory mechanisms of triptolide, the principal active diterpenoid from the Chinese medicinal herb Tripterygium wilfordii Hook. f. Drugs R D. 2003;4(1):1-18. doi:10.2165/00126839-200304010-00001
34. Chiou TT, Chau YY, Chen JB, Hsu HH, Hung SP, Lee WC. Rapamycin attenuates PLA2R activation-mediated podocyte apoptosis via the PI3K/AKT/mTOR pathway. Biomed Pharmacother. 2021;144:112349. doi:10.1016/j.biopha.2021.112349

35. Mei XD, Cao YF, Che YY, Li YF, Wang Y, Gao Y, et al. Danshen: a phytochemical and pharmacological overview. Chin J Nat Med. 2019;17(1):59-80. doi:10.1016/s1875-5364(19)30010-x
36. Tang Y, Zhang Y, Li L, Xie Z, Wen C, Huang L. Kunxian capsule for rheumatoid arthritis: inhibition of inflammatory network and reducing adverse reactions through drug matching. Front Pharmacol. 2020;11:485. doi:10.3389/fphar.2020.00485
37. Ma Z, Liu Y, Li C, Zhang Y, Lin N. Repurposing a clinically approved prescription Colquhounia root tablet to treat diabetic kidney disease via suppressing PI3K/AKT/NF-kB activation. Chin Med. 2022;17(1):2. doi:10.1186/s13020-021-00563-7
38. Zhang Y, Jin D, Kang X, Zhou R, Liu H, Li J, et al. Signaling pathways involved in diabetic renal fibrosis. Front Cell Dev Biol. 2021;9:696542. doi:10.3389/fcell.2021.696542